Developing an experimental strategy to investigate stress-strain models using kaolin

Mair E. W. Beesley[1] MEng, Paul J. Vardanega[2] PhD and Erdin Ibraim[3] PhD

[1]PhD Student, Department of Civil Engineering, University of Bristol, Bristol, United Kingdom
mb0126@bristol.ac.uk
[2]Senior Lecturer, Department of Civil Engineering, University of Bristol, Bristol, United Kingdom
p.j.vardanega@bristol.ac.uk
[3]Reader, Department of Civil Engineering, University of Bristol, Bristol, United Kingdom
Erdin.Ibraim@bristol.ac.uk

ABSTRACT: Prediction of ground movements requires a reliable estimation of soil representative stress-strain behaviour. To do this an assessment of in-situ ('preshear') conditions and the associated influence on the average mobilised soil strength and strain is needed. While many studies focus on undrained shear strength, less effort has been reported for soil shear strain in the context of foundation design. The influence of different experimental and prediction techniques to determine representative soil shear stress-strain design parameters is worthy of study. In this paper, new experimental data is presented of from a series of triaxial and oedometer tests on kaolin. The results demonstrate increasing values of normalised undrained shear strength and reference shear strain with increasing *OCR*.

INTRODUCTION

When designing geo-structures in fine-grained soils, assessing the average resistance and displacement across a mechanism during undrained shear is challenging due to the uncertain influences of previous stress history and subsequent directions of applied shear stress. If a representative stress-strain curve is required, a triaxial test can be used to mimic the in-situ stress and drainage conditions during shear (e.g. Bishop and Henkel 1957). Reconsolidating anisotropically to the in-situ stresses arguably yields a better estimate of in-situ soil parameters (Bjerrum 1973); however, isotropic consolidation is more commonly encountered in practice since the procedure is simpler and less expensive. Bjerrum (1973) recommended that samples should be tested in the laboratory under a variety of test modes (Triaxial compression, UC, Triaxial extension, UE, Direct Simple Shear, DSS) and the undrained shear strengths (c_u) obtained compared to those from field vane tests. Many researchers have investigated the variation in c_u with stress history and direction (Jamiolkowski et al. 1985; Ladd and Foott 1974) but little guidance on similar assessments for soil strain is available.

RESEARCH OBJECTIVES

In this paper, new experimental data of reconstituted kaolin samples which have been tested under various conditions of consolidation and undrained shear are presented. The influence of varying initial void ratio and consolidation rate on the derived

compressibility parameters (λ and κ) in one-dimensional (K_0) and isotropic conditions is investigated. In addition, the bilogarithmic representation (Butterfield 1979) of the compression data is used to derive analogous λ^* and κ^* parameters. The sensitivity of measured stress-strain behaviour and strength to different undrained shearing conditions is examined using alternative representations of the experimental data. The values of strength and strain parameters from each sheared sample are shown to be affected by the assumed shape of sample deformation.

For foundation design, engineers may need to predict the variation in shear strain and c_u for a range of overconsolidation ratio (*OCR*). To model the changes in c_u due to changing *OCR* the formulation based on that presented in Ladd et al. (1977) (Equation 1) is used in this paper. Mayne (1980) compiled a comprehensive database of experimental evidence which supports the validity of Equation 1 for a range of soils.

$$\frac{\left(\frac{c_u}{p'_0}\right)_{OC}}{\left(\frac{c_u}{p'_0}\right)_{NC}} = OCR^{\wedge} \tag{1}$$

Strength mobilisation of fine-grained materials may be characterised using a simple power law (Vardanega and Bolton 2011, Vardanega et al. 2012) (Equation 2):

$$\frac{1}{M} = \frac{\tau_{mob}}{c_u} = 0.5\left(\frac{\gamma}{\gamma_{M=2}}\right)^b \qquad 0.2<\tau_{mob}/c_u<0.8 \tag{2}$$

For serviceability calculations, Equation (2) can be used to predict shear strains where $\gamma_{M=2}$ and b are model parameters calculated from shear stress-strain data (Vardanega and Bolton 2011). Vardanega et al. (2012) presented a correlation (Equation 3) between $\gamma_{M=2}$ and *OCR* using overconsolidated kaolin samples sheared in triaxial compression:

$$\gamma_{M=2} = 0.0040(OCR)^{0.680} \qquad n = 18,\ R^2 = 0.815 \tag{3}$$

METHOD

The kaolin material used in this study was obtained from two different suppliers, identified as Batch 1 and Batch 2 in this research. Table 1 shows the mean and range of measured Atterberg limits and specific gravity for each batch of kaolin. Liquid limit (w_L) was measured using the fall cone penetrometer and the thread-rolling test was used to measure plastic limit (w_P) as per the requirements given in BSI (1990). Specific gravity (*Gs*) was measured using the standard pyknometer method, following the procedure specified in BSI (1990).

Sampling procedure

The sampling procedure for kaolin triaxial samples was developed from the method described by Bialowas (2016). For all triaxial and oedometer tests, powdered kaolin was initially oven-dried for approximately 12 hours which was subsequently cooled for 3 to 4 hours. This was followed by hand mixing into a slurry at the water content

of 130% before curing overnight. Air bubbles were removed from the cured slurry by applying vacuum seated on a vibrating table typically over a period of 2 hours.

For the triaxial samples, the de-aired slurry was then poured into a 50mm-diameter consolidometer and compressed with three increments of vertical pressure to reach the maximum sampling consolidation stress. 'CIUC-1-b-200' and 'CIUC-1-b-404' were further 'swelled' to OCR=2 in the consolidometer prior to extrusion (although negligible height change was observed during the swelling stage, which was most likely due to large shaft friction mobilised in the tall consolidometer). The extruded sample height was designed to be 100mm for each triaxial test (a range of 96-102mm could be achieved). For oedometer samples, the de-aired slurry was poured directly into the oedometer ring.

Triaxial test procedure

Table 2 presents the experimental details of the seven triaxial tests presented in this paper. Two linear voltage displacement transducers (LVDTs) were attached to the top and base caps (Figure 1) to measure axial strain during consolidation and shear and, in particular, to monitor the change in distance between the attached bender elements reliably. For brevity, the bender test results are not discussed in this paper. Owing to the low strength of the reconstituted clay samples, mid-height LVDTs attached directly to the middle section of the sample were judged to be inappropriate. The local strain measurements will be affected by any bedding of the caps; however, for fine-grained materials, the bedding error is likely to be low (Sarsby et al. 1980).

To achieve saturation, the cell and back pressures were raised simultaneously at a rate of 25 to 50kPa/hour. Owing to the uncertain effect on p' during extrusion, which could not be measured from apparently inconsistent measurements of residual pore pressure, different values of effective stress were applied during saturation for each test. The changes in void ratio and axial strain during the saturation period are included in Table 2. With the exception of sample 'CIUC-2-b-200', minimum B values of 0.947 were achieved (Skempton 1954 defines the B value).

Samples were isotropically-consolidated using two continuous stress-controlled loading rates of (a) *8*kPa/hour, and (b) 5kPa/hour. Identifiers (a) and (b) are included as part of each test reference, shown in Table 2. In addition, one isotropic consolidation test ('CI-1') was carried out using discrete increments of total stress with 24-hour drainage intervals. All samples were sheared undrained using a conventional displacement-control frame at a rate of 0.002mm/minute. Assessment of membrane restraint was conducted according to the method of Lade (2016): the order of magnitude of stress contribution is between 1 and 5%. However, the original values of stress are presented in this paper.

Effects of sample tilt

The triaxial samples were observed to develop varying degrees of tilt during isotropic consolidation. This led to 2 potential concerns: (1) misalignment of the LVDTs, resulting in loss of local strain data and, more pertinently, in the restraint on sample

deformation if the LVDT rods became stuck; (2) misalignment of the load cap connection prior to shear.

To alleviate some of the effects of (1) and (2), the sampling procedure was adapted to produce samples with a lower initial void ratio, with the aim of reducing volumetric compression before undrained shear. To reduce the risk of interference between the LVDTs and sample deformation during the test, the original LVDT connection system was replaced with smooth, lightweight components and a wider range of movement. 'Flat' load cap connections (see the descriptions in Table 2) were used for most tests and a photograph of this connection type is shown in Figure 1. Any tilt causes some eccentricity of the axial load applied onto the flat surface. A concave surface was manufactured into the top cap for 'CIUC-2-b-200' to observe the difference in behaviour when the load cap was forced into vertical axial alignment when commencing shear.

To undertake extension tests in the conventional triaxial cell, two cap designs using vacuum chambers were investigated: 'Vacuum-1' consists of a rigid vacuum chamber fixed to the internal load cell, which connects to a smooth Perspex plate on the top cap via vacuum seal (see Figure 2); the second iteration of this component is the rotationally flexible extension cap ('Vacuum-2'), that was designed to accommodate up to 12 degrees of tilt (however, 'CIUC-1-b-403' was tested in compression using this particular cap because a vacuum seal could not be achieved for extension shear due to leakage through the cap joints).

Oedometer testing

Table 3 presents the details of the three oedometer tests undertaken for this study. For tests 'O-1.35' and 'O-1.50', the conventional oedometer was used i.e. a one-dimensional consolidation device with fixed o-ring. Fixed increments of load were applied every 24 hours and vertical displacements were monitored with LVDTs. Test 'O-2.10' was undertaken using a similar setup with the load applied via a stress-controlled triaxial frame.

EXPERIMENTAL RESULTS

Compressibility of isotropic samples

Figure 3 shows the compression data plotted in semi-logarithmic form of the samples undergoing isotropic consolidation. The test data exhibit a pronounced curve in each test, which indicates that every sample had swelled during saturation to a lower effective stress than it had previously experienced. As expected, the apparent preconsolidation stress observed in Figure 3 is somewhat lower than the stress applied in the consolidometer. For example, Sukolrat (2007) measured in reconstituted Bothkennar samples a loss in applied stress of 35-55% on account of consolidometer side friction. From the data presented in Figure 3, it is possible to distinguish samples which had been preconsolidated at higher stresses in the consolidometer ('CIUC-1-b-200', 'CIUC-1-b-403', and 'CIUC-2-b-200').

The results displayed in Figure 3 suggest that initially identical kaolin samples will not

converge to the same normal consolidation line in the stress range studied. The lack of convergence may be due to differences in swelling during saturation. The value of λ shown in Table 4, obtained by linear regression for each test for stresses generally greater than 200kPa, varies from 0.124 to 0.258 and increases with the value of void ratio measured at the end of saturation. As expected, the same pattern emerges with values of λ^* (obtained from Figure 4), although a smaller range is observed.

There appears to be no clear trend in swelling behaviour of the four overconsolidated samples (OCR=2 and 8). Values of κ vary from 0.019 to 0.045 and all samples underwent considerable volume change. The observed changes in void ratio in samples 'CIUC-2-a-208' and 'CIUC-2-b-403' are similar over the same stress range (400 to 200kPa) despite having different swelling rates. However, the swelling lines for the samples overconsolidated using the same procedure to OCR=8 are markedly different; in particular, 'CIUE-8-a-52' appears to continue to consolidate (or leak) at the end of the swelling period.

Compressibility of K_0 (oedometer) samples

Figure 5 shows the compression behaviour of the oedometer samples represented in semi-logarithmic form. The samples tested at higher initial water content exhibit a slightly upward concave shape, indicated by the differences in gradient between the dashed and full lines (corresponding values of λ are provided in Table 4). Since the samples were compressed in the oedometer directly from a slurry, no 'preconsolidation' stress is observed. Values of λ for stresses greater than 60kPa are very similar, varying from 0.235 to 0.247 with high R^2 and *RD* values (Table 4). Although the number of oedometer tests is limited, the data suggests that K0-swelling behaviour is dependent on maximum consolidation stress i.e. κ increases with σ'_{vm} and varies from 0.037 to 0.070.

Behaviour of samples undergoing shear

Figures 7-10 present the behaviour of triaxial samples during strain-controlled undrained shear. From observations of each sample during the shearing stage, little bulging/necking occurred in all cases. The data shown in Figures 7, 8, and 10 were therefore analysed using the assumption of right cylinder deformation (Bishop and Henkel 1957). The resulting parameters are included in Table 5 and the corresponding values for parabolic (bulging/necking) deformation are shown for comparison. Local strain measurements were used for 0-0.5% axial strain in the stress-strain analysis for every test.

The effective stress paths of the kaolin samples, shown in Figure 7, follow patterns reasonably consistent with isotropically-consolidated samples at different values of *OCR* (see Wroth and Loudon 1967 for a similar study). The normalised excess pore pressures generated in the normally consolidated samples (Figure 9) exceed those measured in the lightly overconsolidated (*OCR*=2) samples, resulting in a more pronounced curve in effective stress path prior to peak failure. Stress paths for pairs of samples consolidated in a similar manner (CIUC-1-a-395, CIUC-1-b-403, and CIUC-2-a-208, CIUC-2-b-200) are close in shape although some differences are observed in

mean effective stress and peak deviator stress. The effective stress behaviour of the overconsolidated (OCR=8) samples correspond with the development of negative excess pore pressures; although the sample sheared in extension appears to show an increased tendency to dilate.

The data in Figure 8 illustrate the effect of overconsolidation on the stress-strain behaviour and peak undrained shear strength, with higher values of deviator stress reached at higher values of OCR. Additionally, the increments in stress measured up to around ε_a = 4% are very similar for each pair of samples consolidated in a similar manner (CIUC-1-a-395, CIUC-1-b-403, CIUC-2-a-208, and CIUC-2-b-200). Figure 10 highlights the differences in mobilised strain between tests: if CIUC-2-b-200 is considered to be anomalous (due to substantial bedding which occurred at the start of shear), it appears that strain to failure increases with increasing OCR. The influence of overconsolidation on mobilised strain appears to be dominant at high values of stress ratio (τ_{mob}/c_u>0.5).

Figure 11 shows that the strength ratio (taken as the maximum value of deviator stress normalised by p'_0) of isotropically-consolidated undrained compression (CIUC) tests appears to increase with OCR. Following Equation 1, the parameter Λ obtained by regression is 0.60 (for $(c_u/p'_0)_{NC}$=0.19, n=6 and R^2=0.92), which falls within the range of Λ (0.130-0.998) observed by Mayne (1980) and is slightly lower than the average value (0.70) found for CIUC tests on a variety of soils (Mayne 1988). While the strength ratios of compression tests measured in this study are slightly lower than those found from CIUC tests on similar kaolin material (Vardanega et al. 2012), the values of Λ are similar. Figure 11 also shows the single CIUE test for comparison.

In Figure 12, the deformation parameter $\gamma_{M=2}$ for each test is presented to examine the effect of overconsolidation on measured shear strain. The results indicate that mobilised shear strain increases with OCR, which agrees with the positive trend found by Vardanega et al. (2012) for similar tests on another kaolin material.

DISCUSSION

Influence of test conditions

Figure 3 and Table 4 suggest that values of λ are sensitive to initial void ratio for isotropic samples. A smaller range in λ is observed for the oedometer tests when compared to isotropic data, given the same range in initial void ratio. The rate of isotropic consolidation appears to have relatively little influence on measured compressibility parameters.

Examination of the stress paths in Figure 7 and normalised stress-strain curves in Figure 10 reveal that the large strain behaviour of CIUC-2-b-200 may have been significantly affected by bedding at the start of shear. A ‘concave’ load cap was used, which caused sudden displacement and changes in measured load when axial alignment was forced in the early stages of undrained shearing. The use of a rotationally flexible load cap, however, appears to have little influence on the

mobilised strains (observed in Figure 10) measured in undrained compression- although some differences in the effective stress behaviour are noticeable in Figure 7.

Influence of data representation for test analysis
Comparison of the isotropic compression data (triaxial) shown in Figures 3 and 4 reveals that the bilogarithmic representation yields no apparent increase in linearity. The coefficients of determination for the deduced parameters of λ and λ^* and κ and κ^* are almost identical for this dataset. However, replotting the oedometer data from Figure 5 in bilogarithmic form (as suggested by Butterfield 1979) in Figure 6 produces an apparent increase in linearity. The regression equations shown in Figure 6 indicate that the bilogarithmic representation of K_0 compression data can adequately model the full stress range for each test (10-200 and 10-2000 kPa).

During undrained shear of a triaxial sample, the deformation shape is commonly assumed to be either cylindrical or parabolic, due to the variable influence of frictional end restraint. Table 5 provides the values of parameters for strength (c_u) and strain ($\gamma_{M=2}$) for each triaxial test deduced using the assumption of cylindrical or parabolic sample shape. In compression tests, the parabolic assumption estimates up 5% reduction in strength compared to employing the assumption of right cylinder; while up to 17% reduction is observed in $\gamma_{M=2}$. The extension strength is calculated to be 5% greater with necking than the value calculated assuming cylindrical deformation; similarly, $\gamma_{M=2}$ increases by 9% with the same assumption. This suggests that the strength and strain parameters used in design calculations may be affected by the assumed shape of the sample during shear.

Figures 3 and 5 demonstrate considerable differences in behaviour between oedometer and isotropic samples of similar material. If different values of λ and κ for each of the isotropic and K0 test series are selected as 'representative' compressibility parameters, the deviation in predicted c_u can be estimated using Equation 1 in combination with Equation 4 (which is based on critical state soil mechanics i.e. Schofield and Wroth 1968) of the form shown in Muir Wood (1990):

$$\Lambda = \frac{\lambda - \kappa}{\lambda} \tag{4}$$

Table 6 shows that the chosen 'representative' values of Λ vary slightly between isotropic and K_0 test data. These values of Λ, calculated using Equation 4, are considerably higher than the value (0.60) obtained by regression of measured undrained shear strength ratios (shown in Figure 11). It is possible that the lower value of Λ obtained using Equation 1 may be due a lower than expected c_u value for the OCR=8 compression test.

CONCLUSIONS

The following conclusions are observed from the experimental results in this paper:

- The results of compression tests suggest that isotropic consolidation parameters are sensitive to initial void ratio, possibly due to varying degrees of

swelling during saturation. Values of λ and κ from oedometer tests on non-preconsolidated material are less sensitive to initial void ratio and demonstrate an increase in linearity when represented in bilogarithmic form.

- From a small number of triaxial samples sheared in compression, it appears that the type of load cap connection can have a significant influence on the large strain behaviour of kaolin samples.
- Up to 5% and 17% variation in observed c_u and $\gamma_{M=2}$ can arise from the assumption of sample deformation shape (cylindrical versus parabolic)
- The variations of strength ratio and shear strain with overconsolidation ratio appear to be described by positive trends, which agree with the results of similar, previously published tests on kaolin.

ACKNOWLEDGMENTS

The first author would like to express her appreciation for the help and support she received from the late Dr David Nash. The first author also gratefully acknowledges the DTP scholarship provided by the University of Bristol. The authors thank Mr. Gary Martin for his technical services and support.

NOTATION LIST

The following notation is used in this paper:

B = Skempton's B-value;
b = an exponent (Equation 2);
CIUC = isotropically consolidated undrained compression test;
CIUE = isotropically consolidated undrained extension triaxial test;
c_u = undrained shear strength;
e_m = void ratio measured at the end of consolidation under p'_m;
e_0 = void ratio measured at the end of consolidation under p'_0;
Δe_{PRE} = change in void ratio measured while the load was held "pre-shear" i.e. between the end of consolidation (and swelling) and the start of shearing;
Δe_{SAT} = change in void ratio during sample saturation;
G_S = specific gravity;
n = number of data points in a series or regression;
nc = normally consolidated;
OCR = overconsolidation ratio;
oc = overconsolidated
p' = mean effective stress;
p'_m = maximum mean effective stress during consolidation;
p'_0 = mean effective stress after swell back;
p'_{sat} = mean effective stress during sample saturation;
q = deviator stress;
R^2 = coefficient of determination of a correlation;
RD = relative deviation (as defined in Waters and Vardanega 2009);
v = specific volume;
w_L = liquid limit;
w_P = plastic limit;

γ = shear strain, (1.5 times the axial strain (ε_a) is used in this paper);
$\gamma_{M=2}$ = shear strain mobilised at $0.5c_u$;
ε_a = axial strain;
$\varepsilon_{a\ SAT}$ = axial strain measured from extrusion to the end of saturation
κ = slope of swelling line in semi-logarithmic space;
κ^* = slope of swelling line in bilogarithmic space;
Λ = an exponent (Equation 1);
λ = slope of normal compression line in semi-logarithmic space;
λ^* = slope of normal compression line in bilogarithmic space;
σ'_{vm} = maximum past effective vertical stress in the ground;
σ'_{v0} = vertical effective stress in the ground;
τ_{mob} = mobilised shear stress.

REFERENCES

Bialowas, G. (2016) Time and stress dependent mechanical properties of reconstituted chalk. PhD thesis, University of Bristol, Bristol, United Kingdom.

Bishop, A. W. and Henkel, D. J. (1957). The measurement of soil properties in the triaxial test. Edward Arnold, London, United Kingdom.

Bjerrum, L. (1973). Problems of soil mechanics and construction of soft clays and structurally unstable soils (collapsible, expansive and others). General report, Session four. In: Proceedings 8th International Conference on Soil Mechanics and Foundation Engineering, Moscow (August 6-11, 1973), 3, 111–159.

BSI (1990). Methods of test for soils for civil engineering purposes. British standard BS1377. British Standards Institution, London, United Kingdom.

Butterfield, R. (1979). A natural compression law for soils (an advance on e–log p′). Géotechnique, 29(4), 469-480, https://doi.org/10.1680/geot.1979.29.4.469.

Cerato, A, B. and Lutenegger, A. J. (2004). Determining Intrinsic Compressibility of Fine-Grained Soils. Journal of Geotechnical and Geoenvironmental Engineering, 130(8), 872-877, https://doi.org/10.1061/(ASCE)1090-0241(2004)130:8(872).

Jamiolkowski, M., Ladd, C. C., Germaine, J. T., and Lancellotta, R. (1985). New Developments in Field and Laboratory Testing of Soils. State of the Art, In: Proceedings of the 11th International Conference on Soil Mechanics and Foundation Engineering (San Francisco 12-16th August 1985) pp. 57-153.

Ladd, C.C., and Foott, R. 1974. A new design procedure for stability of soft clays. Journal of the Geotechnical Engineering Division (American Society of Civil Engineers), 100(7), 763–786.

Ladd, C., Foot, R., Ishihara, K., Schlosser, F. and Poulos, H. (1977). Stress-deformation and strength characteristics. In Proceedings of the 9th International Conference on Soil Mechanics and Foundation Engineering, Tokyo, 2, 421–494.

Lade, P. V. (2016). Triaxial testing of soils. John Wiley & Sons Ltd, Chichester, United Kingdom.

Mayne, P. W. (1980). Cam-Clay predictions of undrained strength. Journal of the Geotechnical Engineering Division (American Society of Civil Engineers), 106(11), 1219-1242.

Mayne, P. W. (1988). Determining OCR in clays from laboratory strength. Journal of Geotechnical Engineering (American Society of Civil Engineers), 114(1), 76-92, https://doi.org/10.1061/(ASCE)0733-9410(1988)114:1(76).

Muir Wood, D. (1990). Soil behaviour and critical state soil mechanics. Cambridge University Press, Cambridge, United Kingdom.

Sarsby, R. W., Kalteziotis, N., and Haddad, E. H. (1980). Bedding error in triaxial tests on granular media. Géotechnique, 30(3), 302-309, https://doi.org/10.1680/geot.198 0.30.3.302

Schofield, A. N. and Wroth, C. P. (1968). Critical state soil mechanics. McGraw-Hill Maidenhead, United Kingdom.

Skempton, A. W. (1954). The pore-pressure coefficients A and B. Géotechnique, 4(4), 143- 147, https://doi.org/10.1680/geot.1954.4.4.143.

Sukolrat, J. (2007). Structure and destructuration of Bothkennar clay. PhD thesis, University of Bristol, Bristol, United Kingdom.

Vardanega, P. J. and Bolton, M. D. (2011). Strength mobilization in clays and silts. Canadian Geotechnical Journal, 48(10), 1485–1503, https://doi.org/10.1139/t11-052 and Corrigendum, 49(5), 631, https://doi.org/10.1139/t2012-023.

Vardanega, P. J., Lau, B. H., Lam, S. Y., Haigh, S. K., Madabhushi, S. P. G., and Bolton, M. D. (2012). Laboratory measurement of strength mobilisation in kaolin: link to stress history. Géotechnique Letters 2(1), 9–15, https://doi.org/10.1680/geolett.12.00003.

Waters, T. J. and Vardanega, P. J. (2009). Re-examination of the coefficient of determination (r2) using road materials engineering case studies. Road and Transport Research, 18(3), 3-12.

Wroth, C. P. and Loudon, P. A. (1967). The correlation of strains within a family of triaxial tests on overconsolidated samples of kaolin. In Proceedings Geotechnical Conference, Oslo, pp. 159-163.

TABLES

Table 1. Classification test results

KAOLIN		w_L (%)			w_P (%)			G_S		
Reference	Relevant tests	Mean	*n*	Range	Mean	*n*	Range	Mean	*n*	Range
This study Batch1	O-1.35									
	O-1.50	66.8	4	0.2	35.1	2	0.5	n/a (2.60 assumed)		
This study Batch2	All other tests	65.5	1	-	33.2	2	0.2	2.60	2	0.01
Cerato & Lutenegger (2004)	Oedometer	42	-	-	26	-	-	2.68	-	-
Vardanega et al (2012)	CIU	62.6	1	-	29.6	4	-			

Table 2. Triaxial test details - isotropic consolidation and undrained shear –

Triaxial Test:	CI_1	CIUC-1-a-395	CIUC-2-a-208	CIUC-8-a-51	CIUE-8-a-52	CIUC-1-b-200	CIUC-1-b-403	CIUC-2-b-200
Max. applied stress in sampling device (kPa)	60	60	60	60	60	120	120	120
Extruded w_x (%)	66.0	63.1	59.8	64.1	62.5	54.2	52.7	54.3
Saturation								
Duration (days)	2.18	1.06	1.20	2.15	1.24	0.75	1.01	1.13
p'_{sat} (kPa)	6	4	20	7.5	5	35	34	60
Δe SAT	0.012	0.069	-0.068	0.089	0.290	-0.012	0.014	-0.038
ε_a SAT (%)	1.410*	-0.053	-0.010	-0.005	-0.187	-0.203	0.313	2.137[a]
B value	0.947	0.949	0.952	0.959	0.971	0.958	0.947	0.914
Consolidation								
Loading type	Discrete	8kPa/h	8kPa/h	8kPa/h	8kPa/h	5kPa/h	5kPa/h	5kPa/h
Increments	6	1	3	2	2	4	7	11
Duration (days)	10.21	5.89	3.45	2.95	2.76	8.08	4.88	4.69
Swelling								
Duration (days)	0	0	1.10	4.01	6.13	0	0	10.08
Preshear held stress [b]								
Duration (days)	3.01	0.73	0.05	2.19	4.30	6.19	1.23	7.42
Δe PRE	-0.004*	-.014	0.000	+.006	-.047	-.007	-.008	+.005
e_m	1.142*	1.195	1.158	1.155	1.274	1.236	1.109	1.142
e_0	1.142*	1.195	1.180	1.254	1.271	1.236	1.109	1.159
p'_m (kPa)	395.69	395.16	401.80	399.35	399.85	200.41	403.15	399.87
p'_0 (kPa)	395.47	395.16	208.04	51.30	51.73	200.12	403.15	200.08
OCR	1.0	1.0	1.9	7.8	7.7	1.0	1.0	2.0
Shear mode	Excluded	UC	UC	UC	UE	UC	UC	UC
Load cap		Flat	Flat	Flat	Vacuum-1	Flat	Vacuum-2	Concave
Filter strips		Yes	Yes	Yes	No	No	No	No

Notes: All samples from Kaolin Batch 2; all sheared samples tested with displacement rate = 0.002mm/minute.
[a] The sample came into contact with the load cell during setup
[b] Duration of effective stress held prior to shear; this is included in the consolidation or swelling durations
*Estimated values assuming an extruded sample height of 100mm

Table 3. Oedometer test details

Oedometer Test ID	Batch No.	w_x	σ'_{vm}	σ'_{v0}	No. Increments	Loading Type	Duration Consolidation	Duration Swelling	Duration Total
		%	kPa	kPa			days	days	days
O-1.35	1	90.0	400	20	9	Discrete	6	3	9
O-1.50	1	99.2	400	20	9	Discrete	6	3	9
O-2.10	2	138.2	2000	100	20	Discrete	8	6	14
Cerato & Lutenneger (2004)									
*O-1.00		42.0	786	786	15	Discrete	15	0	15
*O-1.25		52.5	778	778	15	Discrete	15	0	15
*O-1.50		63.0	786	786	15	Discrete	15	0	15
*O-1.75		73.5	786	786	15	Discrete	15	0	15

*Tests from the literature included for comparison

Table 4. Calculated compressibility parameters

Test ID	Stress range kPa	*n*	λ	R^2	*RD*	λ*	R^2	*RD*	Stress range kPa	*n*	κ	R^2	*RD*	κ *	R^2	*RD*
Isotropic consolidation																
CI-1	200-400	3	0.208	.999	3.2	0.094	.999	3.2								
CIUC-1-a-395	200-400	3	0.206	1.00	0	0.093	1.00	0								
CIUC-2-a-208	200-400	3	0.164	.999	3.2	0.072	.999	3.2	400-200	3	0.034	.990	10.0	0.015	.990	10.0
CIUC-8-a-51	200-400	5	0.195	1.00	0	0.083	1.00	0	400-51	8	0.045	.993	8.19	0.020	.994	7.8
CIUE-8-a-52	200-400	3	0.258	1.00	0	0.105	1.00	0	400-52	5	0.023	.892	32.9	0.010	.892	32.9
CIUC-1-b-200	100-200	3	0.124	1.00	0	0.052	.999	3.2								
CIUC-1-b-403	200-400	5	0.127	.990	10.0	0.058	.990	10.0								
CIUC-2-b-200	200-400	5	0.141	.999	3.2	0.062	.999	3.2	400-200	5	0.019	.927	27.0	0.009	.928	26.8
Vardanega et al. (2012)																
*Average of 4 tests			0.250								0.039					
K0 (oedometer) consolidation																
O-1.35	10-60	4	0.237	.998	4.6	0.084	.997	5.9								
	60-200	3	0.247	.997	5.8	0.100	.998	4.2	200-20	4	0.037	.981	13.6	0.016	.983	13.2
O-1.50	10-60	4	0.272	.998	4.7	0.094	.999	2.8								
	60-200	3	0.249	.997	5.7	0.099	.998	4.1	200-20	4	0.039	.989	10.6	0.016	.990	10.1
O- 2.10	10-60	3	0.339	.998	4.0	0.114	.999	1.0	100/400	5	0.057	.935	25.6	0.025	.932	26.0
	60-2000	8	0.231	.999	1.7	0.105	.998	4.6	2000-100	7	0.070	.997	5.7	0.036	.995	7.1
Cerato & Lutenegger (2004)																
*O-1.00	153-786	5	0.069	0.998	4.5	0.036	.998	4.1								
*O-1.25	153-778	5	0.079	0.998	4.5	0.042	.999	3.2								
*O-1.50	153-786	5	0.088	0.997	5.5	0.045	.998	4.5								
*O-1.75	152-786	5	0.091	0.999	3.2	0.046	1.0	0								

*Tests from the literature included for comparison

Table 5. Summary of state and shear parameters

Triaxial Test:	CIUC-1-a-395	CIUC-1-b-200	CIUC-1-b-403	CIUC-2-a-208	CIUC-2-b-200	CIUC-8-a-51	CIUE-8-a-52
λ	0.206	0.124	0.127	0.164	0.141	0.195	0.258
κ	-	-	-	0.034	0.019	0.045	0.023
Λ	-	-	-	0.793	0.865	0.769	0.911
p'_0	395.16	200.12	403.15	208.04	200.08	51.3	51.73
OCR	1.0	1.0	1.0	1.9	2.0	7.8	7.7
Right cylinder							
c_u (kPa)	68.25	43.63	75.41	65.90	69.12	30.62	-25.49
c_u/p'_0	0.17	0.22	0.19	0.32	0.35	0.60	0.49
p'_{peak} (kPa)	197.14	111.00	216.18	166.89	155.57	68.76	57.89
M	0.69	0.79	0.70	0.79	0.89	0.89	-0.88
$\varepsilon_{a\ peak}$ (%)	4.97	6.05	5.63	6.16	10.49	7.58	-9.24
$\gamma_{M=2}$	0.0032	0.0025	0.0051	0.0049	0.0053	0.0123	0.0146
b	0.335	0.263	0.406	0.341	0.293	0.416	0.413
Parabolic bulging or necking							
c_u (kPa)	66.66	42.48	73.43	64.04	65.71	29.49	-26.69
c_u/p'_0	0.17	0.21	0.18	0.31	0.33	0.57	0.52
p'_{peak} (kPa)	202.29	112.32	219.25	169.26	154.05	67.83	57.09
M	0.66	0.76	0.67	0.76	0.85	0.87	-0.94
$\varepsilon_{a\ peak}$ (%)	4.40	5.32	4.98	5.36	9.83	7.23	-9.24
$\gamma_{M=2}$	0.0030	0.0022	0.0048	0.0046	0.0045	0.0114	0.0161
b	0.339	0.263	0.413	0.344	0.305	0.412	0.412

Table 6. Derived parameters for c_u prediction (right cylinder assumed)

Consolidation and swelling parameters derived from:	Isotropic compression (Average)	(n)	K_0 compression	Measured c_u (Equation 1)
λ	0.160	(6)	0.231	-
κ	0.033	(3)	0.057	-
Λ	0.795		0.753	0.60

FIGURES

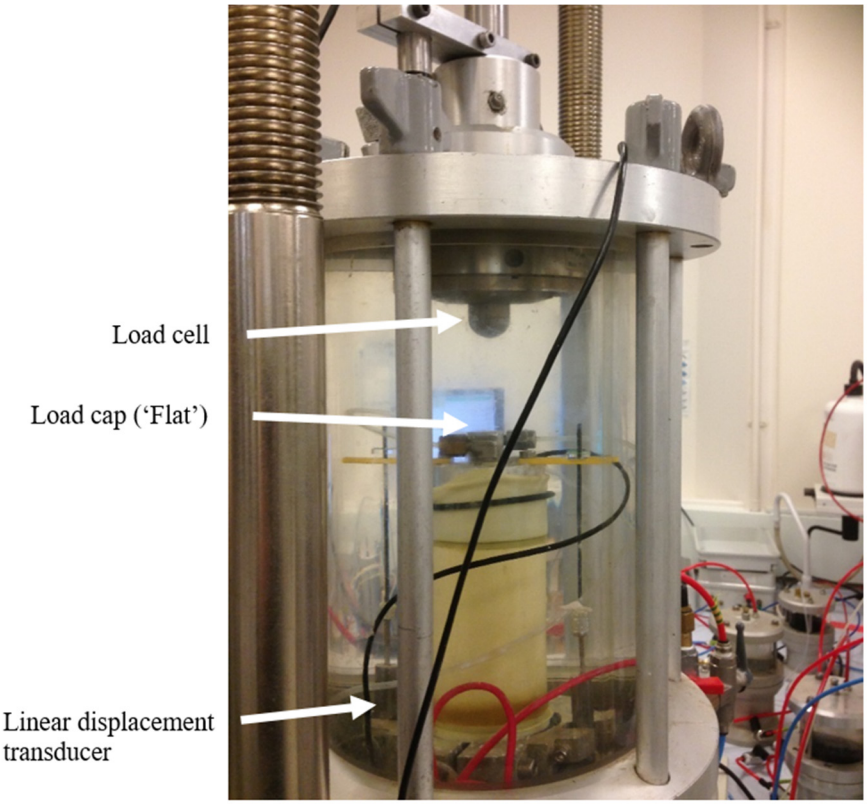

FIG.1. Compression test setup of kaolin inside conventional isotropic triaxial cell (Linear displacement transducers are attached to the base and top caps with a lightweight connection system)

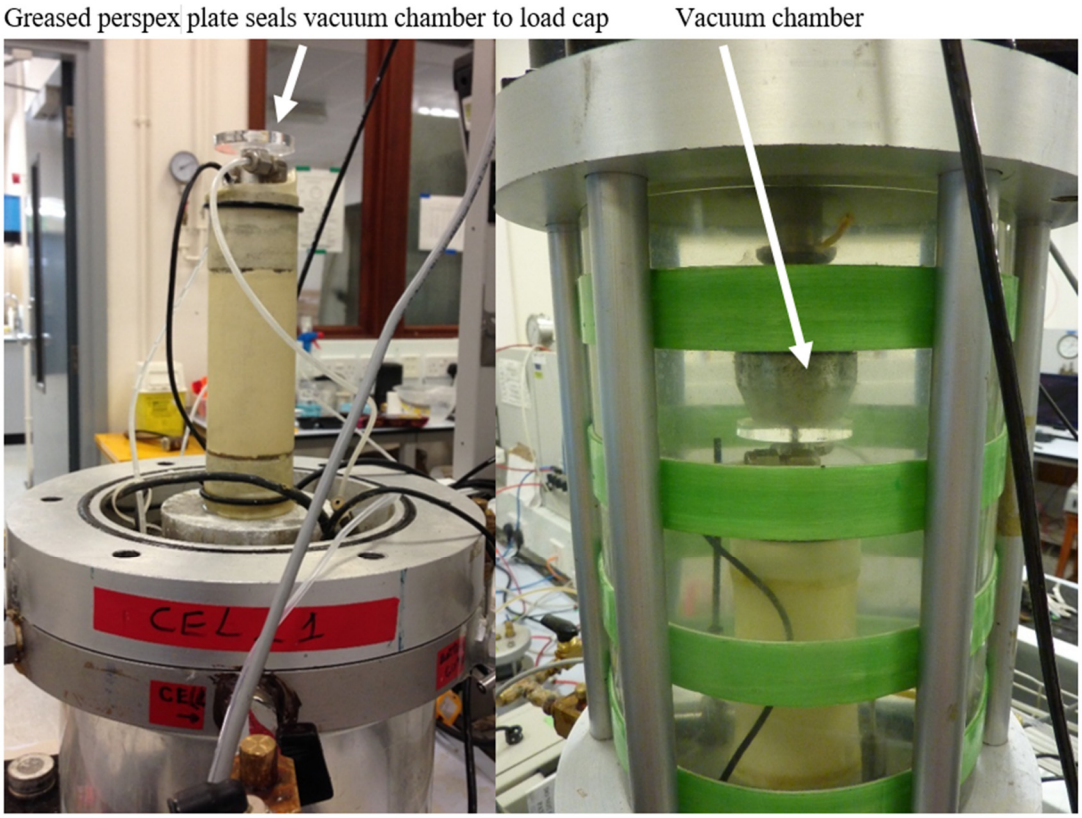

FIG.2. Extension test setup of kaolin sample CIUE-8-1 inside conventional isotropic triaxial cell with extension cap "Vacuum-1"

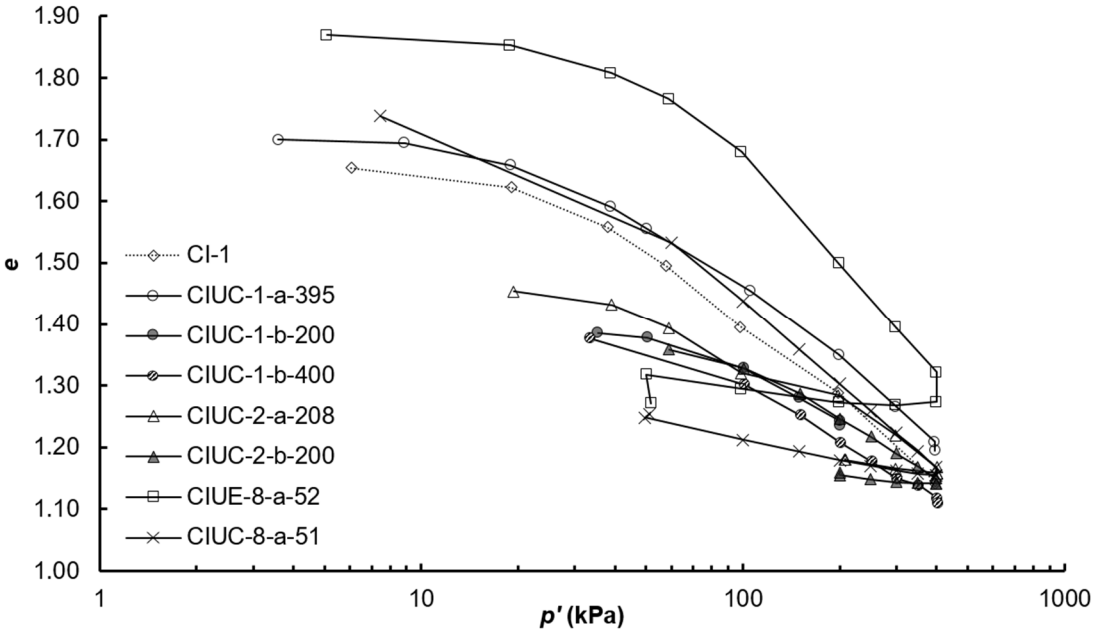

FIG.3. Semi-logarithmic isotropic-consolidation curves of reconstituted kaolin at different initial water content due to swelling during saturation

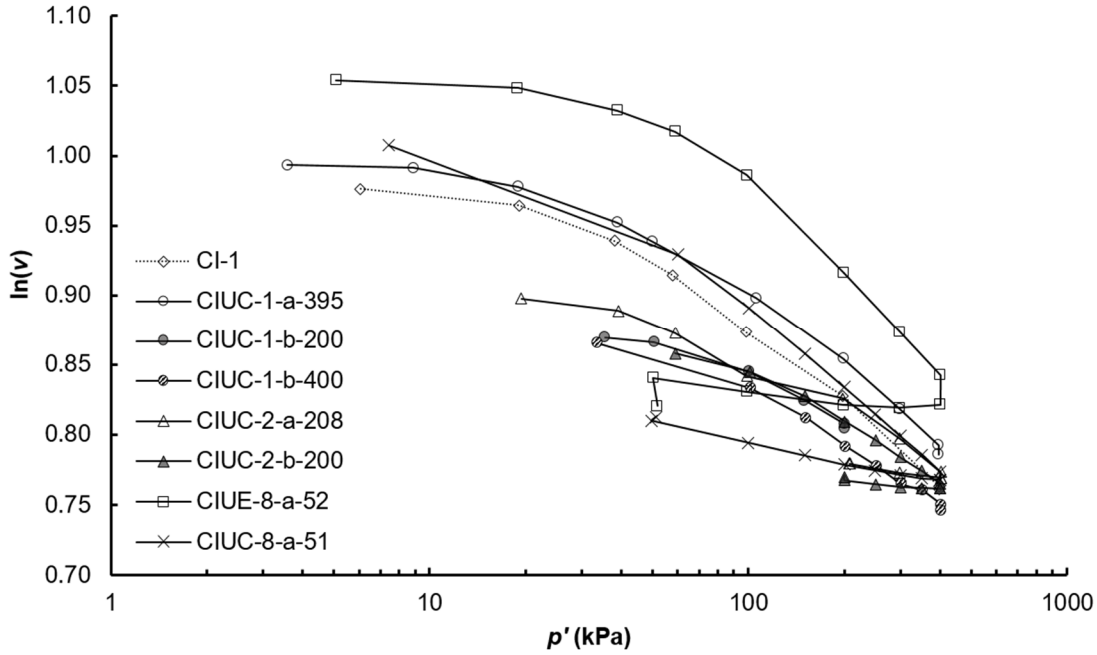

FIG.4. Bilogarithmic isotropic-consolidation curves of reconstituted kaolin at different initial water content due to swelling during saturation

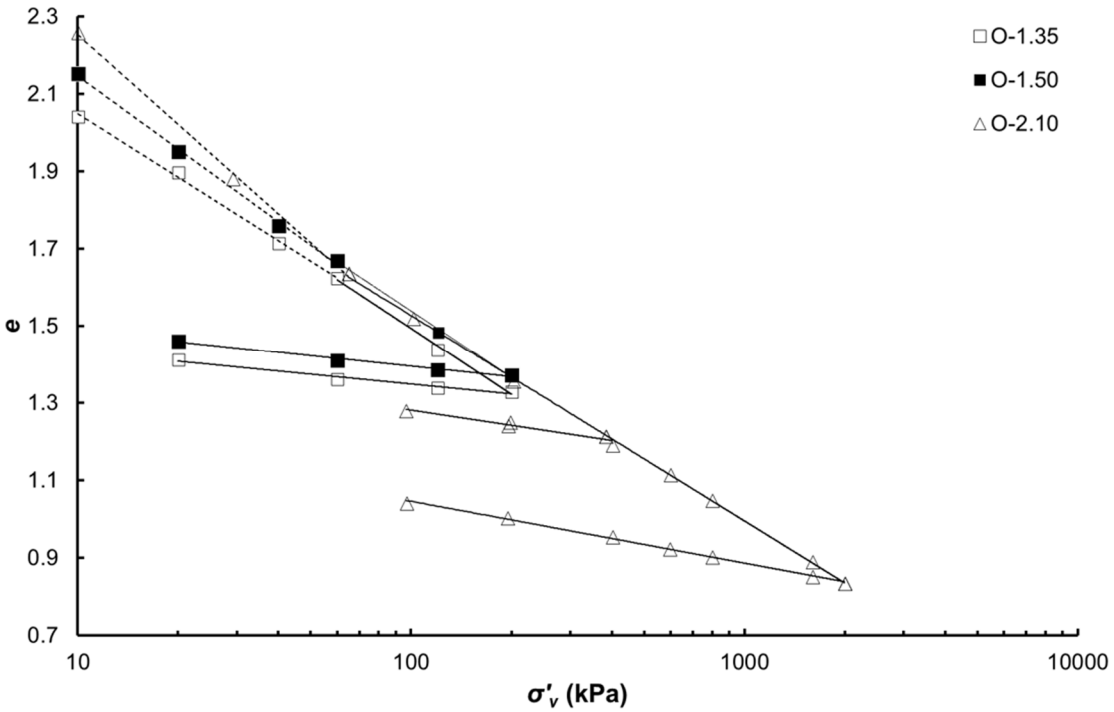

FIG.5. Semi-logarithmic K0-consolidation (oedometer) curves of reconstituted kaolin mixed at different initial water content

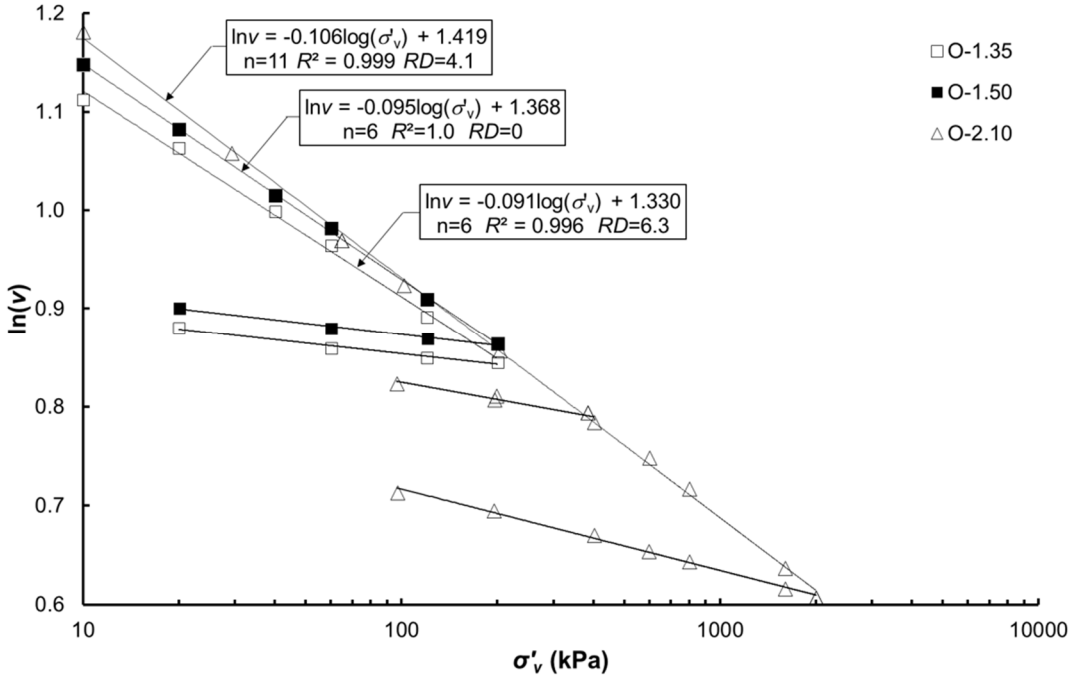

FIG.6. Bilogarithmic K0-consolidation (oedometer) curves of reconstituted kaolin mixed at different initial water content

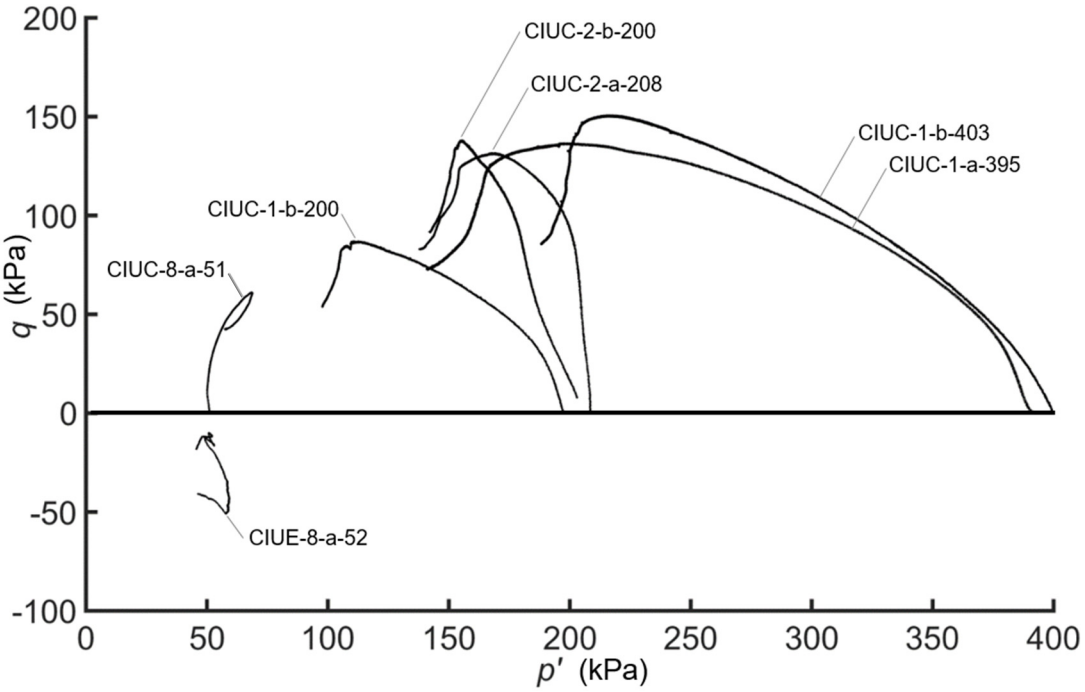

FIG.7. Effective stress paths for isotropically consolidated triaxial samples

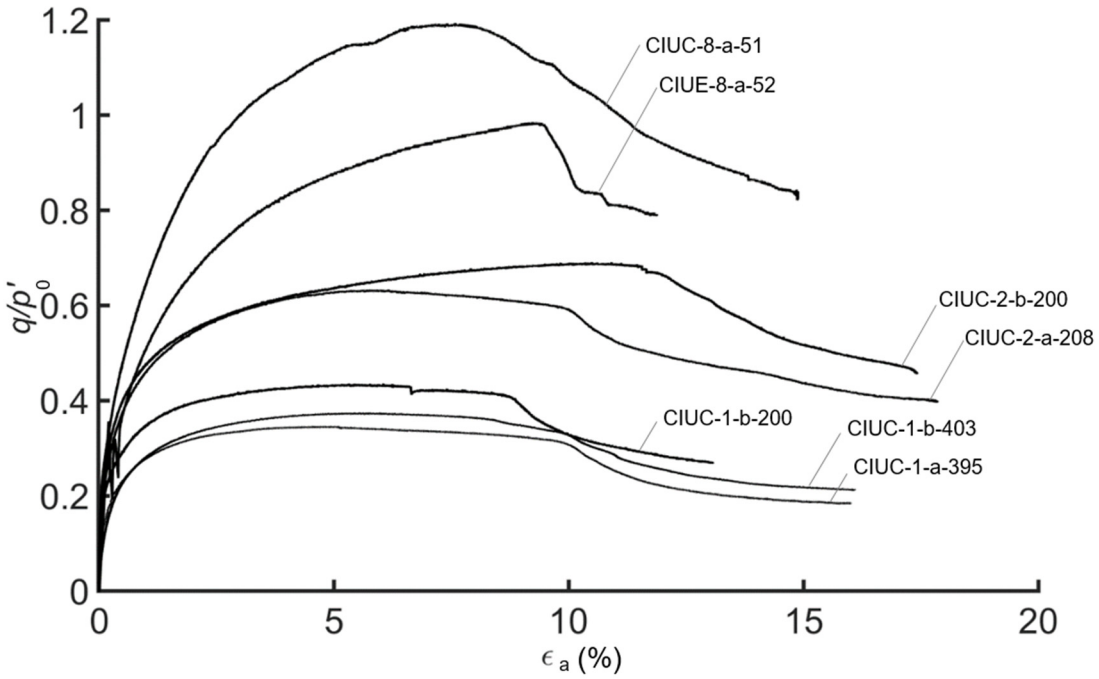

FIG.8. Stress-strain curves for isotropically consolidated triaxial samples – comparison of tests by p'_0 normalisation (assumed cylinder deformation)

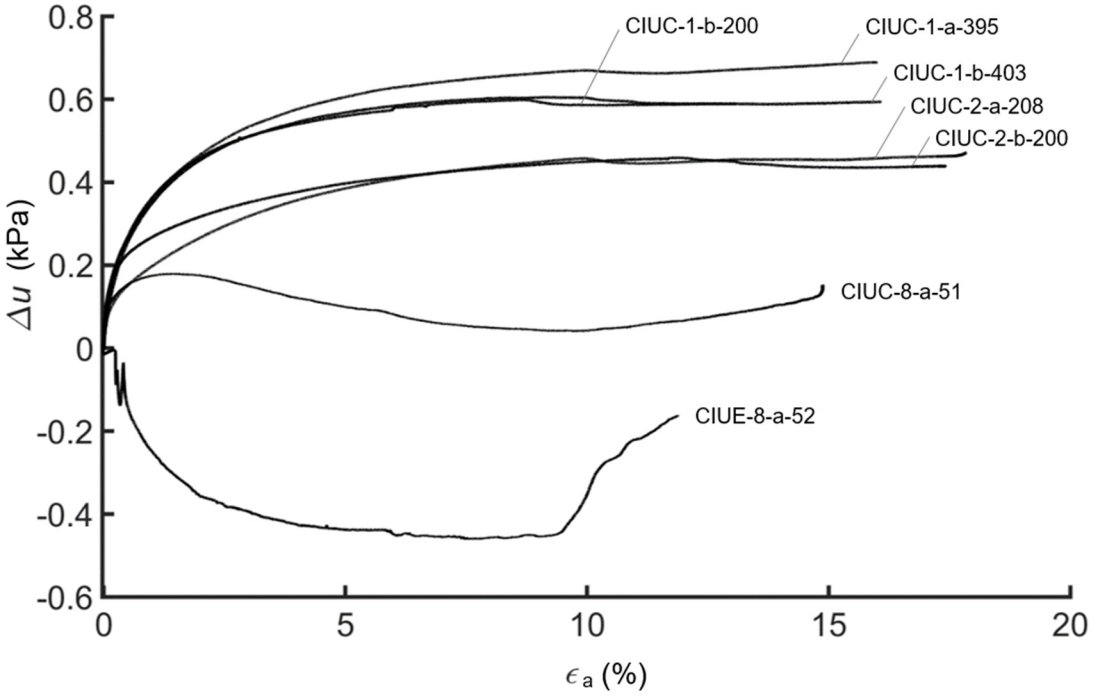

FIG.9. Excess pore pressure-strain curves for isotropically consolidated triaxial samples – comparison of tests by p'_0 normalisation

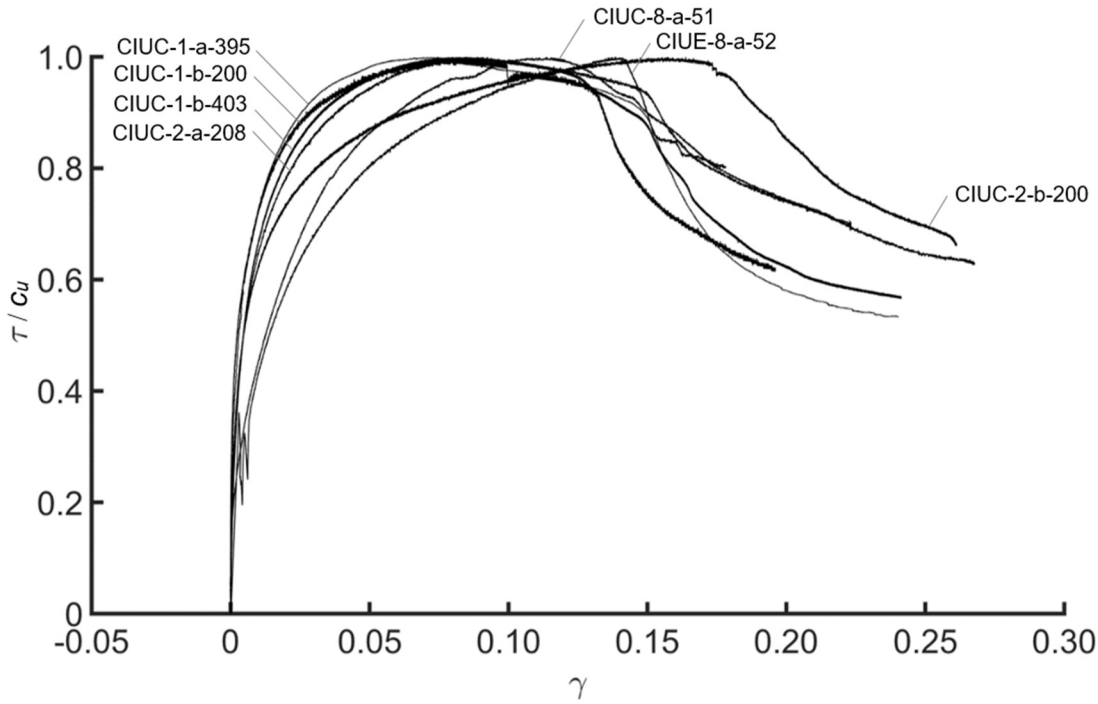

FIG.10. Stress-strain curves for isotropically consolidated triaxial samples – comparison of tests by c_u normalisation (assumed cylinder deformation)

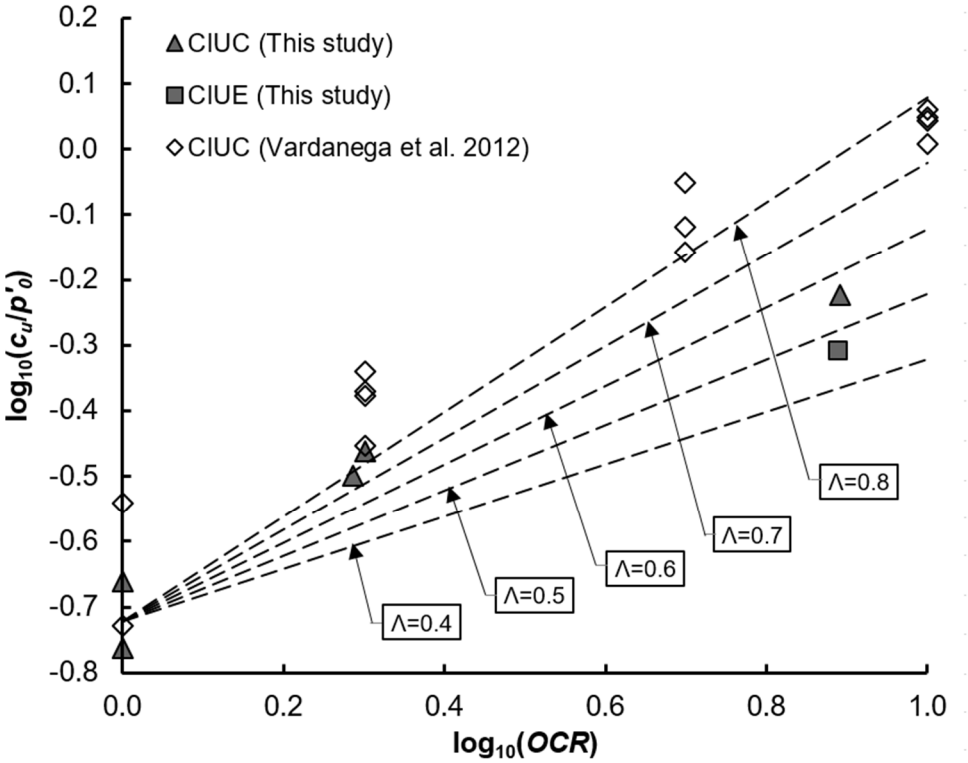

FIG.11. Relationship between undrained shear strength ratio (cylinder) and OCR (following the frameworks of Ladd et al. 1977 and Mayne 1980)

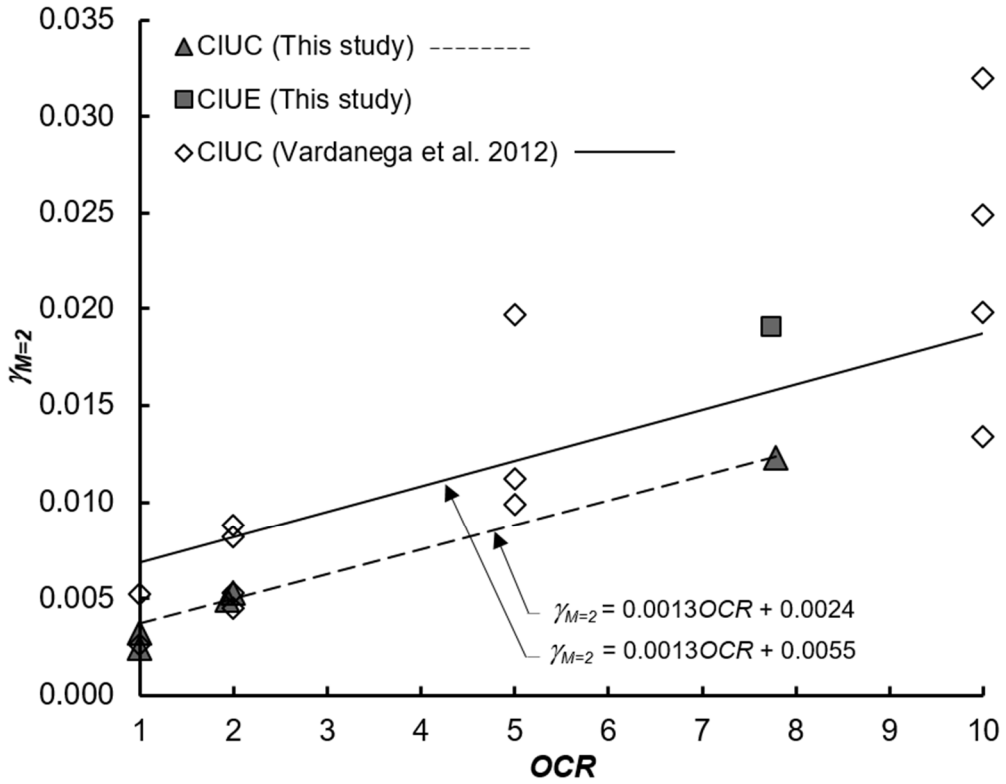

FIG.12. Dependence of deformation parameter $\gamma_{M=2}$ (cylinder) on *OCR* values Values from Vardanega et al. 2012 for *OCR* =15 and 20 not shown but best fit linear line generated using the entire dataset. Best fit line through the new CIUC data from this study does not include the single CIUE test.